ORIGINAL RESEARCH

Sulfonate-modified phenylboronic acid-rich nanoparticles as a novel mucoadhesive drug delivery system for vaginal administration of protein therapeutics: improved stability, mucin-dependent release and effective intravaginal placement

ChunYan Li,[1] ZhiGang Huang,[2] ZheShuo Liu,[1] LiQian Ci,[3] ZhePeng Liu,[3] Yu Liu,[2] XueYing Yan,[1] WeiYue Lu[2]

[1]School of Pharmacy, Heilongjiang University of Chinese Medicine, Harbin, [2]Department of Pharmaceutics, School of Pharmacy, Key Laboratory of Smart Drug Delivery, Ministry of Education, Fudan University, [3]School of Medical Instrument and Food Engineering, University of Shanghai for Science and Technology, Shanghai, People's Republic of China

Correspondence: Yu Liu
Department of Pharmaceutics, School of Pharmacy, Key Laboratory of Smart Drug Delivery, Ministry of Education, Fudan University, Room 815, Research Building, 826 Zhangheng Road, Shanghai 201203, People's Republic of China
Tel/fax +86 21 5198 0090
Email liuyu@fudan.edu.cn

XueYing Yan
School of Pharmacy, Heilongjiang University of Chinese Medicine, 24 Heping Road, Harbin 150040, Heilongjiang, People's Republic of China
Tel/fax +86 451 8219 3038
Email 15159267@qq.com

Abstract: Effective interaction between mucoadhesive drug delivery systems and mucin is the basis of effective local placement of drugs to play its therapeutic role after mucosal administration including vaginal use, which especially requires prolonged drug presence for the treatment of gynecological infectious diseases. Our previous report on phenylboronic acid-rich nanoparticles (PBNPs) demonstrated their strong interaction with mucin and mucin-sensitive release profiles of the model protein therapeutics interferon (IFN) in vitro, but their poor stability and obvious tendency to aggregate over time severely limited future application. In this study, sulfonate-modified PBNPs (PBNP-S) were designed as a stable mucoadhesive drug delivery system where the negative charges conferred by sulfonate groups prevented aggregation of nanoparticles and the phenylboronic acid groups ensured effective interaction with mucin over a wide pH range. Results suggested that PBNP-S were of spherical morphology with narrow size distribution (123.5 nm, polydispersity index 0.050), good stability over a wide pH range and 3-month storage and considerable in vitro mucoadhesion capability at vaginal pH as shown by mucin adsorption determination. IFN could be loaded to PBNP-S by physical adsorption with high encapsulation efficiency and released in a mucin-dependent manner in vitro. In vivo near-infrared fluorescent whole animal imaging and quantitative vaginal lavage followed by enzyme-linked immunosorbent assay (ELISA) assay of IFN demonstrated that PBNP-S could stay in the vagina and maintain intravaginal IFN level for much longer time than IFN solution (24 hours vs several hours) without obvious histological irritation to vaginal mucosa after vaginal administration to mice. In summary, good stability, easy loading and controllable release of protein therapeutics, in vitro and in vivo mucoadhesive properties and local safety of PBNP-S suggested it as a promising nanoscale mucoadhesive drug delivery system for vaginal administration of protein therapeutics.

Keywords: mucoadhesion, phenylboronic acid, stability, controlled-release, protein therapeutics, nanoparticles

Introduction

Prolonged local placement of mucosal drug delivery system and the maintenance of adequate local drug level are favorable irrespective of administration route,

local therapy or systemic absorption.[1] This offered special significance for vaginal administration, which is necessary in the case of contraception, treatment of yeast infection, hormonal replacement therapy, feminine hygiene and so on. However, insufficient interaction of the drug with mucosa and the overlaying mucus, which leads to short local placement, is the main obstacle for conventional mucosal formulations, which lead to the development of mucoadhesive drug delivery systems[2] that usually interact with mucin, which is the main component of mucus as well as mucosal membranes.[3,4] For example, as one of the most widely used mucoadhesive polymers, chitosan is believed to interact by its positively charged amino groups with the anionic counterpart in mucin (mainly sialic acid) and retain the formulation for extended time periods on the mucosa of the administration site.[5,6] Chitosan gel was reported to demonstrate high mucoadhesiveness, suitable mechanical and release properties with good vaginal retention.[7] Liposomes[8] or liquid crystal precursor mucoadhesive systems[9] decorated with chitosan also achieved obvious in vitro and in vivo mucoadhesion.

Conventional mucoadhesive strategies are mainly based on non-covalent bonds such as hydrogen bonds, van der Waals forces, ionic interactions and even simply physical interpenetration effects. For stronger and longer mucoadhesion, new mucoadhesive strategies relying on covalent bonds with mucin are proposed and investigated. For instance, modification by thiolation in drug delivery systems has been pioneered aiming to form covalent bonds with cysteine-rich subdomains of mucin.[3,10,11] Such chemical modification even further improved the mucoadhesive behavior of conventional mucoadhesive materials as demonstrated by the fivefold increase in the mucoadhesion percentage by thiolated chitosan nanoparticles than non-thiolated chitosan nanoparticles[12]

and enhanced nasal bioavailability by mucoadhesive drug delivery systems based on thiolated carbopol.[13,14]

As an alternative mucoadhesive strategy, phenylboronic acid (PBA) modification is attracting increasing interest for its ability to react with vicinal diol to form a stable cyclic ester[15] that makes possible effective interaction with mucin, which is rich in oligosaccharides. The success of insulin-loaded poly(2-lactobionamidoethyl methacrylate-3-acrylamido phenylboronic acid) micelles for nasal delivery[16] and cyclosporine-loaded PBA-functionalized poly(D,L-lactide)-*b*-dextran nanoparticles for ocular administration[16,17] revealed the potential of PBA modification for mucoadhesion.

Our previous report on phenylboronic acid-rich nanoparticles (PBNPs) preliminarily demonstrated considerable in vitro mucoadhesive properties in a wide pH range including the mild acidic environment and mucin-sensitive release profiles of the model protein therapeutics interferon (IFN).[18] However, the stability of PBNPs is not satisfactory because their tendency to aggregate over time or at neutral pH severely limited manipulation, long-term storage and future expansion of application.

Modification by sulfonate groups is an effective strategy to optimize the hydrophilicity and stability of drug carriers such as sulfobutylether-β-cyclodextrin (commercially available as Captisol®), which was approved as the solubilizing adjuvant for both oral and intravenous administration[19] and widely used in studies on mucosal use.[20,21] For another example, a sulfated polysaccharide fucoidan was reported to effectively stabilize iron oxide nanoparticles in aqueous environment.[22] Therefore, the objective of the present study was to stabilize PBNPs by sulfonate group modification and maintain their drug-loading, drug-releasing and mucoadhesion advantages (Figure 1). Sulfonate group-containing monomers were introduced into the
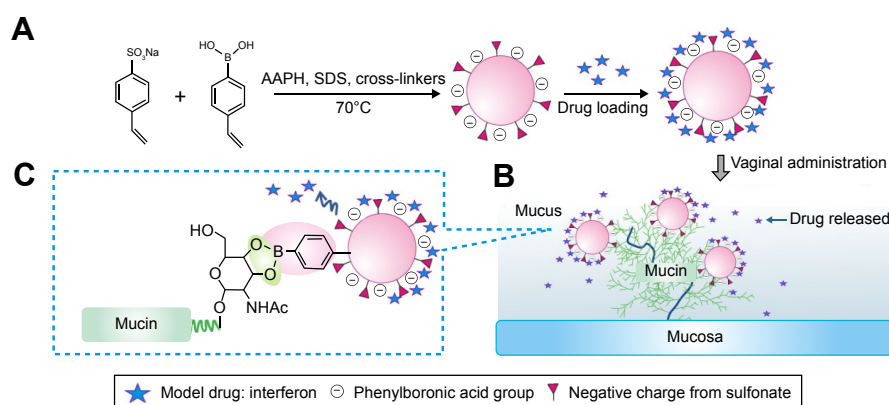
Figure 1 PBNP-S for mucoadhesive drug delivery.
Notes: (**A**) Synthesis and protein therapeutics loading of PBNP-S. The presence of sulfate made PBNP-S negatively charged and more stable in aqueous circumstances. (**B**) Adherence of PBNP-S to mucin present in the mucus and on the surface of mucosa after intravaginal administration. (**C**) Mucoadhesion of PBNP-S based on the formation of reversible covalent complexes between the phenylboronic acid moiety on the PBNP-S and vicinal diols in the mucin molecules.
Abbreviations: PBNP-S, sulfonate-modified phenylboronic acid-rich nanoparticles; AAPH, 2,2′-azobis(2-methylpropionamidine) dihydrochloride; SDS, sodium dodecyl sulfate.

composition of nanoparticles to construct sulfonate-modified phenylboronic acid-rich nanoparticles (PBNP-S) where negative charges in a wide pH range conferred by sulfate groups prevented possible nanoparticle aggregation of nanoparticles and PBA groups that ensured effective interaction between nanoparticles and mucin. PBNP-S were further characterized with respect to stability, interaction with mucin, IFN loading and in vitro release. Then, the in vivo mucoadhesive property of PBNPs and PBNP-S was evaluated in mice with respect to the intravaginal placement of both nanoparticles themselves by near-infrared (NIR) fluorescent whole animal imaging and IFN quantitation by enzyme-linked immunosorbent assay (ELISA) in the vaginal lavage. Finally, the local irritation PBNPs were evaluated.

Materials and methods
Materials
4-Vinylphenylboronic acid (VPBA), sodium dodecyl sulfate (SDS), sodium styrene sulfonate (SSS), *N,N*-methylene bisacrylamide (MBAAm), ethylene glycol dimethacrylate (EGDMA), 2,2′-azobis(2-methylpropionamidine) dihydrochloride (AAPH) and other chemicals were purchased from Aladdin reagent Inc. (Shanghai, People's Republic of China) and used as received. The lyophilized α-IFN was kindly provided by Shanghai United Cell Biotechnology Co. Ltd (Shanghai, People's Republic of China). Fluorescein isothiocyanate (FITC), IR783, bovine serum albumin (BSA) and mucin from porcine stomach (product ID: M2378) were purchased from Sigma-Aldrich (St Louis, MO, USA). Pierce® BCA Protein Assay Kits were purchased from Thermo Scientific (Waltham, MA, USA). The water used in all experiments was of Milli-Q grade (Millipore, Billerica, MA, USA).

Female Institute of Cancer Research mice (21–25 g) were provided by the Shanghai Laboratory Animal Center (Shanghai, People's Republic of China). All animals were allowed free access to standard food and tap water and acclimated for at least 1 week before use. All animal experiments were carried out in accordance with the guidelines evaluated and approved by the Ethics Committee of the School of Pharmacy, Fudan University, and the study was approved by the ethics committee of Fudan University.

Preparation of PBNP-S
PBNP-S were synthesized as described in previous reports[18,23] except that SSS was included in the polymerization at the weight ratio in the total monomers of 5% (the product nanoparticles named as PBNP-S5) and 10% (as PBNP-S10). Briefly, in a 250 mL round-bottom flask equipped with a stirrer (MS-H-Pro + stirrer; Dragon Lab Inc., Beijing, People's

Republic of China) and a N_2 gas inlet, 100 mL SDS solution (0.053%, w/v) was heated to 30°C, followed by the addition of VPBA (0.970 g) and appropriate amounts of SSS, MBAAm and EGDMA under stirring. After 30 minutes, polymerization was initiated by adding 1 mL of 0.105 M AAPH and increasing the temperature to 70°C and then allowed to proceed for 5 hours. The resultant PBNP-S5 or PBNP-S10 suspension was purified by 3 days of dialysis against very frequently changed pure water at room temperature (~22°C). Similarly, IR783-labeled fluorescent PBNPs were synthesized except that IR783 was included (10 mg/20 mL) in the polymerization of nanoparticles. For comparison, PBNPs were also synthesized except that no SSS was included as a monomer.

Characterization of PBNP-S
The morphology of PBNP-S5, PBNP-S10 and PBNPs was observed by transmission electronic microscopy (TEM, 2100F; JEOL Co., Tokyo, Japan). The size distribution and zeta potential of nanoparticles were measured by dynamic light scattering (DLS, Zetasizer; Malvern Co., Malvern, UK). The Fourier transform infrared spectroscopy (FT-IR) spectrum of nanoparticles lyophilized by a freezing dryer (Virtis AdVantage Plus; SP Industries, Warminster, PA, USA) was obtained by Avatar 360 FT-IR (Thermo Fisher Scientific).

Stability of PBNP-S
To investigate the stability of nanoparticles in various pH values, the size distribution and zeta potential of freshly prepared PBNP-S5, PBNP-S10 or PBNPs dispersed in buffers of different pH values (20 mM citrate buffer for pH 4, 5 and 6, while 20 mM phosphate salts for pH 7, 8 and 9) were measured by DLS.

To investigate the long-term stability of various nanoparticles, PBNPs, PBNP-S5 and PBNP-S10 (10 mg/mL) were mixed with buffers of different pH values as described earlier at the volume ratio of 1:10. After standing for 3 months, the size distribution was measured again by DLS. If obvious sedimentation was observed, the supernatant was sampled for analysis.

Adsorption of mucin by PBNP-S
In vitro mucoadhesion of nanoparticles (PBNP-S5, PBNP-S10 and PBNPs) was evaluated by measuring mucin adsorption expressed as the amount of mucin adsorbed per milligram of nanoparticles. Briefly, nanoparticles dispersed in buffers of different pH values (10 mg nanoparticle/mL buffer, 20 mM citrate buffer for pH 4, 5 and 6, while 20 mM phosphate salts for pH 7, 8 and 9) were mixed with mucin solution (0.5 mg/mL) at the volume ratio of 1:1 and incubated at 37°C for 1 hour. The mixture was then centrifuged at 6,950× *g* for

10 minutes (H1650-W centrifuge; Xiangyi Instrument Inc, Changsha, People's Republic of China). Mucin concentration in the supernatant was measured by BCA Protein Assay Kits to calculate the adsorption amount of mucin according to the difference between the initial concentration and the supernatant concentration of mucin. The time profile of the adsorption amount at pH 4 was further measured to evaluate the rate of adsorption.

Drug loading and release

IFN was loaded to PBNP-S or PBNP by the simple physical adsorption. Briefly, a stock solution of IFN was mixed with respective nanoparticle suspension in buffers at the drug:nanoparticle ratio of 1:10 (w/w). This loading process needed only mild shaking by hand for several minutes. The mixture was then centrifuged at $15,637 \times g$ for 15 minutes to collect precipitated IFN-loaded nanoparticles. Unbound IFN was removed by repeated dispersion and centrifugation of as-prepared precipitated IFN-loaded nanoparticles in fresh buffer. All the supernatants were collected to determine the amount of unbound IFN by bicinchoninic acid (BCA) protein assay for calculation of drug loading (DL) and encapsulation efficiency (EE).

In the in vitro release experiment, FITC-labeled IFNs (FITC-IFNs) were used instead as the model protein therapeutics to facilitate the quantitative determination of the low concentration of IFN in the release medium. Release of FITC-IFN was conducted in the vaginal fluid stimulant containing mucin at a physiological level (1.5%, w/v) or without in a shaking bath at 37°C for 3 days.[18] FITC-IFN concentration in the release samples was determined by fluorescent spectrophotometry at E_x 495 nm and E_m 520 nm with a microplate reader (Synergy 2; Bio-Tek Co., Winooski, VT, USA) to calculate the accumulative FITC-IFN release percentage relative to the loading amount at each time point.

NIR fluorescent imaging of the in vivo intravaginal placement of nanoparticles

To evaluate the in vivo intravaginal placement of nanoparticles, 10 μL of IR783-labeled PBNP-S5 or PBNPs dispersion (10 mg/mL) was intravaginally administered to each mouse with a microliter syringe with a blunt needle, which was inserted 2–3 mm into the orificium vaginae. IR783 solution (10 μg/mL in normal saline, of similar fluorescent signal intensity with nanoparticle suspension) was also tested for comparison. NIR fluorescent images were obtained immediately (time 0), 3 hours, 9 hours, 24 hours and 48 hours after administration with a whole-mouse imaging system (IVIS spectrum; PerkinElmer, Santa Clara, CA, USA) at E_x 780 nm and E_m 820 nm.

Quantitative evaluation of the intravaginal presence of IFN released from nanoparticles

To quantitatively evaluate the intravaginal placement of IFN after vaginal administration of IFN-loaded nanoparticles, IFN-loaded PBNP-S5 and PBNPs (prepared as mentioned in the "Adsorption of mucin by PBNP-S" section, pH set at 5) with similar IFN loading (20 μg/mL) were intravaginally administered (10 μL per mouse) as described in the "NIR fluorescent imaging of the in vivo intravaginal placement of nanoparticles" section. IFN solution (20 μg/mL) was also tested as the control group. Every group contained 30 mice, from which five mice were randomly selected at time 0, 3 hours, 9 hours, 24 hours and 48 hours to perform vaginal lavage in which the vagina was thoroughly washed by normal saline. All the vaginal lavage fluid was collected, diluted to 1.00 mL with water and centrifuged to get the supernatant to determine IFN concentration by ELISA (Human Interferon α ELISA Kit; Fu Sheng Industrial Co., Shanghai, People's Republic of China) according to the kit instruction. The amount of resident IFN was expressed as the percentage of total IFN dosage.

Preliminary local irritation evaluation

To examine the impact of PBNP-S on the morphology of vaginal mucosa, three groups of female mice (n=3 per group) were intravaginally administered as described in the "NIR fluorescent imaging of the in vivo intravaginal placement of nanoparticles" section with normal saline, PBNP-S5, IFN solution and IFN-loaded PBNP-S5, respectively. After 24 hours, mice were sacrificed to get vagina tissues for histological examination after hematoxylin and eosin (H&E) staining and photographed by microscopy (DMI4000B; Leica Microsystems, Wetzlar, Germany).

Statistics

The one-way analysis of variance (ANOVA) was used for comparison among groups. Differences of the mean values were evaluated by the Student's unpaired t-test. A $P < 0.05$ was considered statistically significant.

Results
Preparation and characterization of PBNP-S

The preparation method of PBNP-S was similar to that used in our previous publication.[18] Sulfonated monomers were included to confer the product nanoparticles negative charges for better stability. Two types of PBNP-S were prepared, differing in the ratio of sulfonated monomers in the total input amount of monomers and cross-linkers

(PBNP-S5 and PBNP-S10, responding to 5% and 10% w/w, respectively). Both PBNP-S5 and PBNP-S10 were spherical in shape (Figure 2) with narrow size distribution (123.5 nm, polydispersity index [PDI] 0.050 and 143.7 nm, PDI 0.049, respectively) and negatively charged (−30.3 mV and −37.3 mV, respectively). The absorption peaks at 1,068 cm^{-1} and 1,194 cm^{-1} in the FT-IR spectrum of PBNP-S5 and PBNP-S10 may be assigned to the stretching vibration of the sulfonate group (Figure S1).[24]

Improved stability of PBNP-S over PBNP

Tendency of aggregation was used to limit the practical application of PBNPs, which not only significantly aggregated at neutral pH (Figure 2B) but also became bigger and bigger during storage at all tested pH values from 4 to 9 (Figure 3). And that is the main reason why sulfated monomers were introduced into the composition of PBNPs. As expected, both PBNP-S5 and PBNP-S10 demonstrated improved stability over a wide pH range (Figure 2B) and storage (Figure 3B and C) in comparison with PBNPs.

Mucin adsorption

Figure 4A reveals the difference between PBNP-S5 and PBNP-S10. The adsorption amount of PBNP-S5 at various pH values was similar to that of PBNP, while PBNP-S10 only efficiently adsorbed mucin in the pH range 4–6. Even in the range of pH 4–6, the adsorption of mucin by PBNP-S10 was less than that of PBNP and PBNP-S5. All three nanoparticles demonstrated a quick adsorption profile at the typical vaginal pH (Figure 4B).

IFN loading and in vitro release

The model protein therapeutics IFN was effectively adsorbed by all three nanoparticles (PBNP, PBNP-S5 and PBNP-S10) in a pH-dependent manner (Figure 5A). In mild acidic environment (pH 4–6), the adsorption of PBNP-S was comparable to that of PBNP, while in neutral and mild basic environment (pH 7–9), the adsorption of PBNP-S was significantly lower than that of PBNP.

Fluorescent spectrometry was preferred for easier quantitative analysis of the release medium, because BCA assay may be interfered by constituents in vaginal fluid simulants such as glycerol and BSA. Therefore, IFN was fluorescently labeled by FITC via a classical method[25] and loaded onto the three nanoparticles with similar drug loading and encapsulation efficiency (Table S1). As shown in Figure 5B, release of FITC-IFN from PBNP-S at vaginal pH demonstrated a mucin-dependent manner.
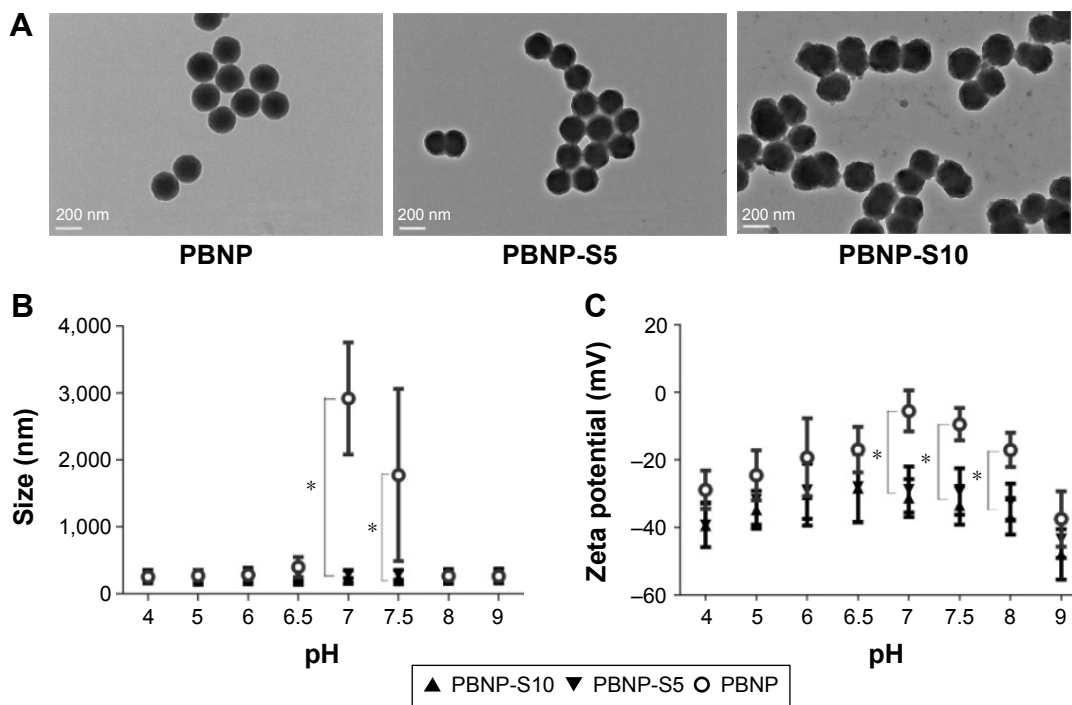
Figure 2 Characterization of PBNP-S.
Notes: (**A**) TEM image of PBNP, PBNP-S5 and PBNP-S10. Scale bars: 200 nm. (**B**) Size distribution of PBNP, PBNP-S5 and PBNP-S10 at different pH values measured by DLS (mean ± distribution width). (**C**) Zeta potential of PBNP, PBNP-S5 and PBNP-S10 at different pH values measured by DLS (mean ± distribution width). *Significantly different.
Abbreviations: PBNP-S, sulfonate-modified phenylboronic acid-rich nanoparticles; PBNPs, phenylboronic acid-rich nanoparticles; PBNP-S5, PBNP-S at a weight ratio of 5%; PBNP-S10, PBNP-S at a weight ratio of 10%; TEM, transmission electronic microscopy; DLS, dynamic light scattering.

Based on the comprehensive consideration of stability, mucin adsorption, IFN loading and release properties, PBNP-S5 was selected for further in vivo evaluation.

Intravaginal placement of PBNP-S

When PBNP and PBNP-S were fluorescently labeled, in vivo imaging tracing became possible. The size distribution and zeta potential of fluorescently labeled nanoparticles are listed in Table S2. Figure 6A shows the difference between the intravaginal placement of nanoparticles and probe solution,

where the former remained in the vagina for >24 hours, and the latter was completely eliminated from the vagina by 24 hours. Both PBNP and PBNP-S5 showed significant advantages in prolonged intravaginal placement.

Local placement of IFN released from PBNP-S5

As shown in Figure 6B, immediate washing after administration could recover ~90% of the IFN dosage for the control group (IFN solution). For PBNP and PBNP-S5, <20% of
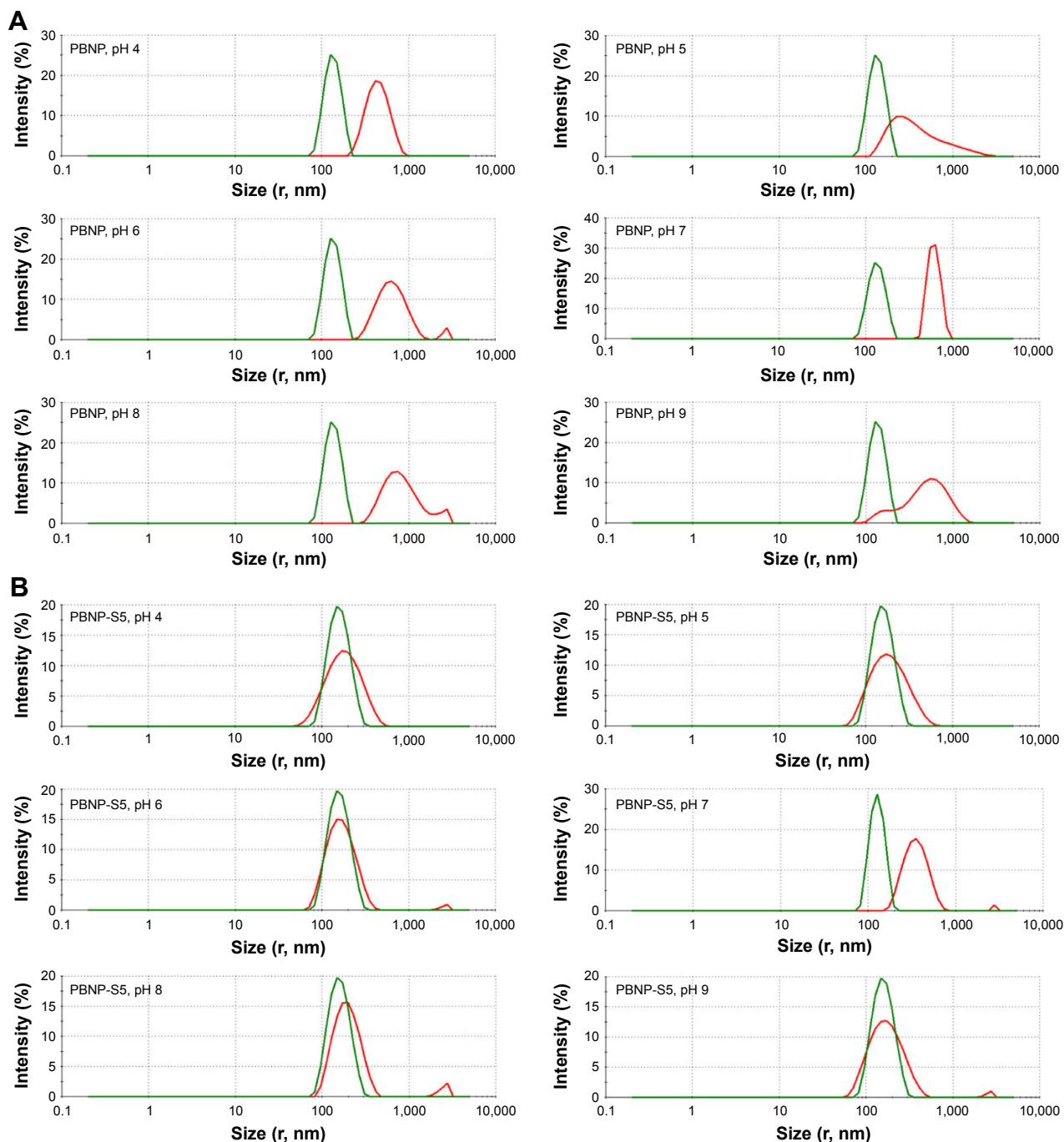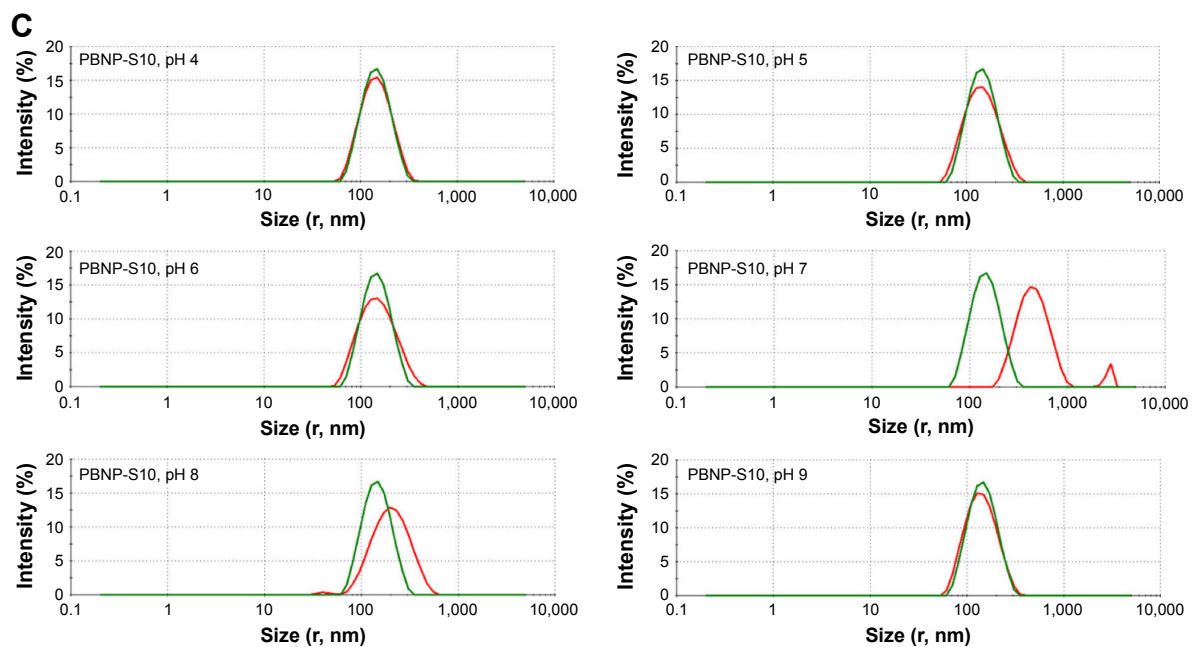

Figure 3 (*Continued*)

C

Figure 3 Change in size distribution of PBNPs (**A**), PBNP-S5 (**B**) and PBNP-S10 (**C**) before and after 3-month storage measured by DLS (green lines: measured in 2–3 days after synthesis and dispersed in pure water and red lines: after storage and dispersed in various buffer).
Abbreviations: PBNPs, phenylboronic acid-rich nanoparticles; PBNP-S, sulfonate-modified phenylboronic acid-rich nanoparticles; PBNP-S5, PBNP-S at a weight ratio of 5%; PBNP-S10, PBNP-S at a weight ratio of 10%; DLS, dynamic light scattering.

the dosage was found to be released at time 0, indicating a very limited extent of in vivo burst release. For the control group, the intravaginal IFN level dramatically decreased with time due to the self-cleaning function of the vagina. In contrast, a considerable intravaginal IFN level was maintained for 24 hours in the PBNP and PBNP-S5 group.

Preliminary local mucosal irritation evaluation

Local mucosal irritation of PBNP-S5 was preliminarily evaluated by histological examination of the vaginal mucosa

of mice after vaginal administration. No obvious histological change in microscopic photographs (Figure 6C) and vaginal irritation scores (Table S3) was observed for both PBNP-S5 and IFN-loaded PBNP-S5, similar to that for normal saline and IFN solution itself. Further systemic evaluation of the local safety of PBNP-S for vaginal use is included in our future plan.

Discussion

Safety, effectiveness and stability have been considered as the most important aspects for formulations. Our previous
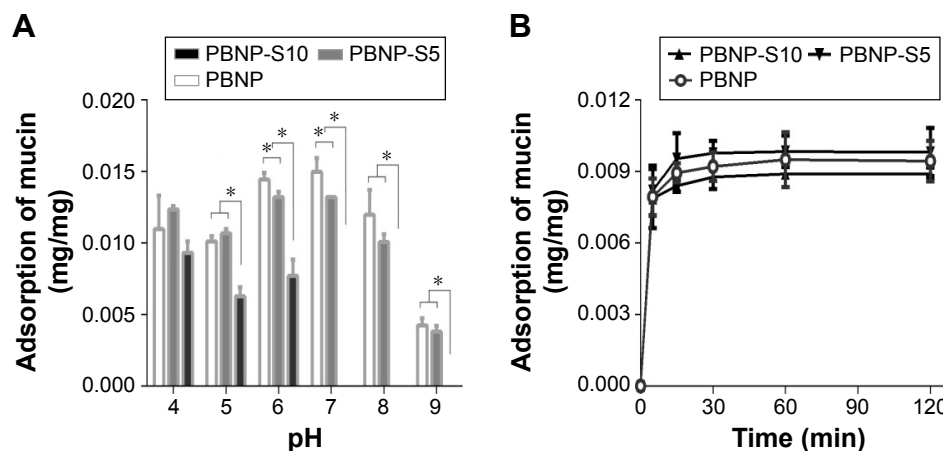
Figure 4 Adsorption of mucin by PBNP, PBNP-S5 and PBNP-S10.
Notes: (**A**) Influence of pH. (**B**) Adsorption kinetics at pH 4 (mean ± SD, n=3). *$P<0.05$.
Abbreviations: PBNPs, phenylboronic acid-rich nanoparticles; PBNP-S, sulfonate-modified phenylboronic acid-rich nanoparticles; PBNP-S5, PBNP-S at a weight ratio of 5%; PBNP-S10, PBNP-S at a weight ratio of 10%; min, minutes.
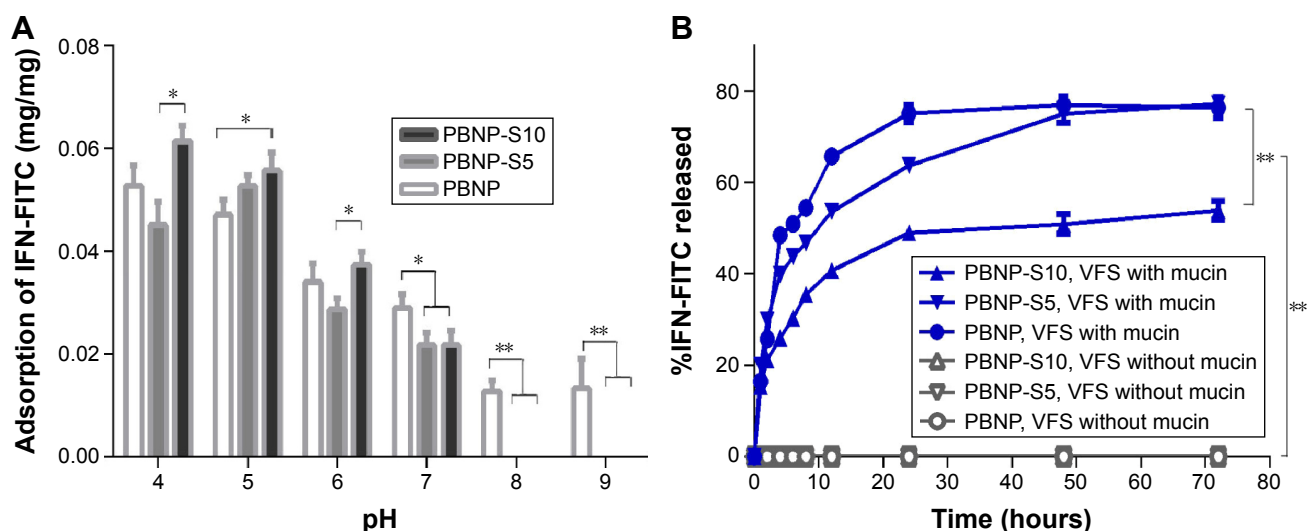
Figure 5 Drug loading and release of sulfated PBNPs with IFN-FITC as the model protein therapeutics.
Notes: (**A**) Adsorption of IFN-FITC by PBNP (white), PBNP-S5 (gray) and PBNP-S10 (black) at different pH values. (**B**) Release of IFN-FITC from PBNP (circle), PBNP-S5 (inverted triangle) and PBNP-S10 (triangle) in VFS with (blue) or without mucin (gray). Mean ± SD, n=3. *$P<0.05$ and **$P<0.01$.
Abbreviations: PBNPs, phenylboronic acid-rich nanoparticles; IFN-FITC, fluorescein isothiocyanate-labeled interferon; PBNP-S, sulfonate-modified phenylboronic acid-rich nanoparticles; PBNP-S5, PBNP-S at a weight ratio of 5%; PBNP-S10, PBNP-S at a weight ratio of 10%; VFS, vaginal fluid simulant; SD, standard deviation.

report on PBNPs preliminarily demonstrated effective in vitro mucoadhesion throughout a wide pH range and controlled release profiles of the model protein therapeutics IFN. However, for nanoparticles with large surface and poor kinetic stability, long-term storage often constitutes a great challenge. In previous experiments, the stability issue of PBNPs was noticed because PBNPs tended to sediment and even cake during storage. Therefore, in the present investigation, modification by sulfonate groups was conducted to optimize the surface wettability, and encouraging results indicating good in vitro and in vivo mucoadhesive properties of PBNP-S were obtained. Taking the improvement in nanoparticle stability into consideration, sulfonate group modification may provide a practical strategy for mucoadhesive drug delivery.

To our knowledge, sulfonate modification has been used to modify biomaterials for improving surface chemistry including increased surface wettability of alkyl sulfonate amphiphile[26] and poly(sodium styrene sulfonate)-grafted Ti_6Al_4V materials.[27] Here, sulfonated monomers were included in the synthesis of nanoparticles to provide stable negative charges as proven by the zeta potential data throughout a wide pH range (Figure 2C), similar to previous literature on improved colloidal stability of poly(styrenesulfonate)-coated nanoparticles assessed through sedimentation tests.[28] In contrast, the zeta potential of PBNP was close to zero in the pH range 7–7.5, in accordance with the aggregation tendency of PBNP in this pH range (Figure 2B) or over storage (Figure 3).

It was worth explaining that the mixtures of nanoparticles with different buffers had been set quietly for 3 months and the sediment on the bottom even began to cake. We tried to redisperse it but found that repeatable redispersion was too difficult to realize, and the size of sedimentation particles was also far beyond the suitable range of DLS. As an alternative approach, the supernatant containing aged particles for both PBNP and PBNP-S was submitted to DLS analysis and could also reveal clearly the difference between PBNP and PBNP-S. PBNP-S5 and PBNP-S10 maintained a stable particle size over the pH range 4 and showed no visible sedimentation over 3-month storage. Only slight tendency of particle size growth was observed for sulfonated PBNPs at pH 7 after 3 months, which might be due to the relatively small potential absolute value at this pH.

In vitro mucin adsorption is an important criterion for mucoadhesive formulations.[29,30] Both PBNP and PBNP-S5 could effectively adsorb mucin, while PBNP-S10 could not. This difference may be ascribed to the presence of too many negative charges on PBNP-S10, which might hinder the accessibility of the negative-charged oligosaccharide side chains of mucin[31] to the PBA groups on nanoparticles. Similar unfavorable influence of negative charge on the adherence between biomaterials and surrounding hydrophobic surfaces[26] and, more importantly, mucoadhesion[32] has been reported in the literature. A recent investigation confirmed the relationship between surface charge and mucoadhesion from another viewpoint by proving in situ mucoadhesion of nanoparticles based on the change in surface charge
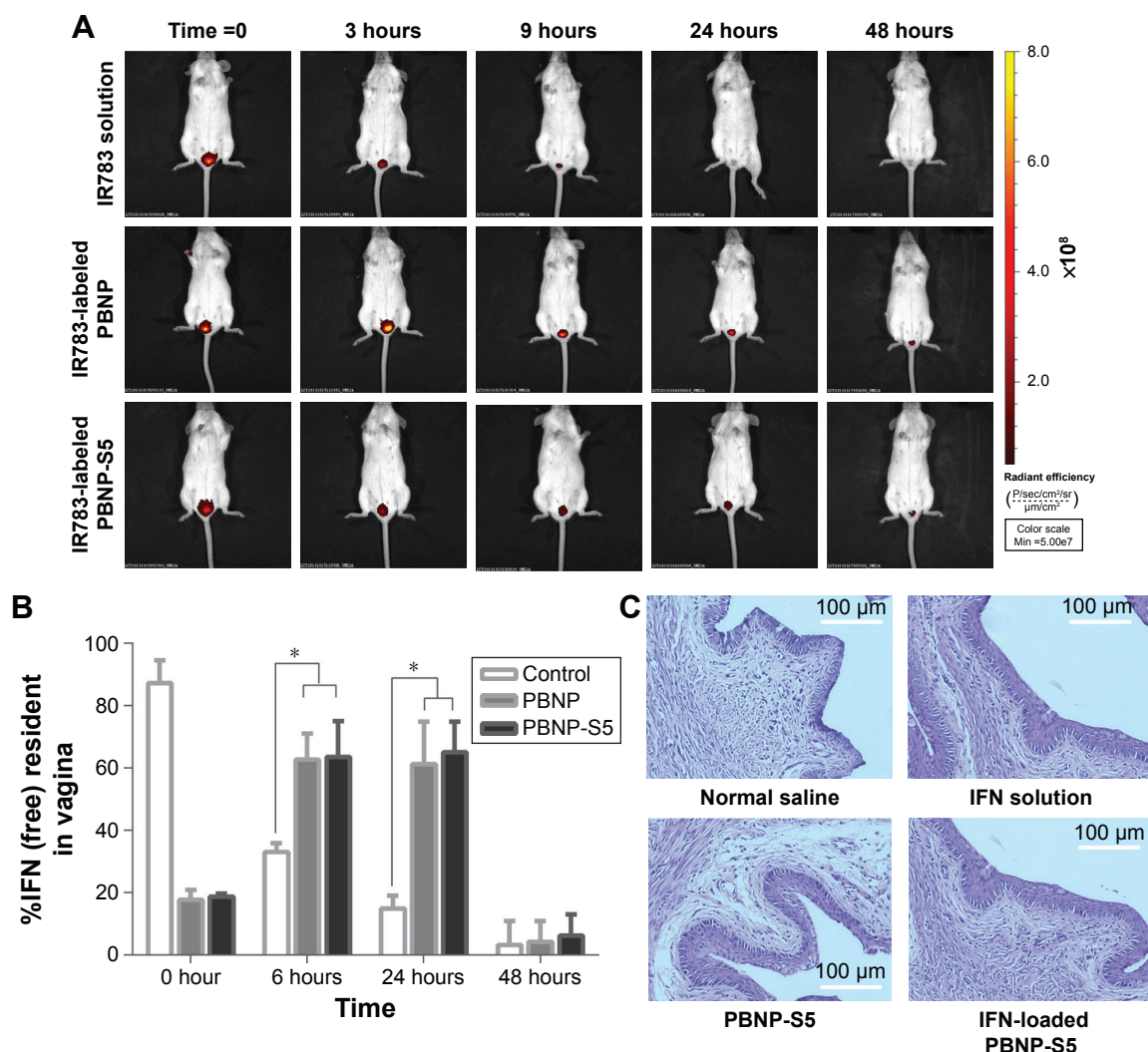
Figure 6 In vivo evaluation of sulfated PBNPs.
Notes: (**A**) Prolonged intravaginal placement of IR783-labeled PBNPs and PBNP-S5 in mice in comparison with IR783 solution demonstrated by in vivo fluorescent imaging in mice. (**B**) Prolonged intravaginal presence of IFN using PBNP and PBNP-S5 as drug delivery systems determined by vaginal washing and ELISA (mean ± SD, n=6). (**C**) Preliminary local irritation evaluation: histological microscopy of vaginal mucosa of mice intravaginally administered with normal saline (negative control), IFN solution, PBNP-S5 and IFN-loaded PBNP-S5. *$P<0.05$.
Abbreviations: PBNPs, phenylboronic acid-rich nanoparticles; PBNP-S, sulfonate-modified phenylboronic acid-rich nanoparticles; PBNP-S5, PBNP-S at a weight ratio of 5%; IFN, interferon; ELISA, enzyme-linked immunosorbent assay; SD, standard deviation.

from negative to positive by in situ enzyme activation on mucosa.[33] Generally speaking, the presence of negative charge on nanoparticles is unfavorable to adhesion to mucin. Fortunately, PBNP-S5 showed mucin adsorption capability similar to PBNP, indicating that sulfonate groups at least did not hamper the mucoadhesive properties of nanoparticles. In other words, the amount of negative charges on PBNP-S5 is more suitable because it balanced well the requirements of stability vs mucoadhesion.

It is worth mentioning that commercially available mucin contains some protein impurities. Here, possible interference from protein impurities was addressed by testing IFN release in the presence of BSA, which is the most possible relevant protein impurity at the same concentration as mucin

(Figure S2). Both PBNP-S5 and PBNP-S10 showed ~10% burst release, much less than that by mucin, indicating that at least the mucin concentration-related release was not totally the result of impurity interference.

α-IFN has been used in the form of creams and hydrogels to treat vaginal flat condyloma as early as 1984. But conventional semi-solid formulations leak quickly from the vagina and usually require repeated administration, practical inconvenience and poor compliance of patients.[18,34] Therefore, IFN was used in the present investigation as the model protein therapeutics to achieve prolonged intravaginal placement and thus better patient compliance. The adsorption of IFN by PBNPs or PBNP-S may be at least partially attributed to electronic interaction. Because the isoelectric point of

IFN is ~pH 6, IFN should be positively charged at pH <6 and easily attracted by the negatively charged PBNP or PBNP-S. At pH >6 (pH 7–9), IFN would be negatively charged and its adsorption by PBNP or PBNP-S will be mainly dependent on hydrophobic interaction, which might be even hindered by the electronic repulsion between the negative charge of IFN and the negative charge on PBNP-S.

The mucin-sensitive profiles from PBNP-S in vaginal fluid simulant were similar to our previous report on PBNP.[18] This phenomenon may be attributed to the steric effect brought by the binding of mucin on PBNP or PBNP-S. Mucin was expected to bind with the PBA groups on nanoparticles via the formation of boron ester, while IFN was more likely to be adsorbed on nanoparticles by electronic interaction as well as hydrophobic interaction. The huge size of mucin constituted steric hindrance to firm adsorption of IFN on the surface of nanoparticles via electronic or hydrophobic interaction. The relatively less release ratio of PBNP-S10 may be related to the less mucin adsorption by PBNP-S10 as discussed earlier. This speculation still need more direct proof in the future.

Considering that vaginal pH may be in a wider range in the case of microbial infections or after intercourse, release of IFN was also characterized at pH 6 (Figure S3) and pH 8 (Figure S4). Release of IFN at pH 6 was also related to the presence of mucin, while obvious burst release even in the release medium without mucin was observed. This may be caused by the difference in the IFN adsorption capacity of nanoparticles at different pH values (Figure 5A) because IFN loading for release experiments at pH 6 or 8 was performed at pH 4 to assure consistency with the release experiment at pH 4. On the other hand, the release profile of IFN at pH 8 was quite different. Almost all IFNs were released immediately for PBNP-S, no matter if there was mucin or not, in agreement with the near-zero IFN adsorption by PBNP-S as shown in Figure 5A. These results may suggest that both PBNP and PBNP-S tended to release IFN when pH was elevated, favoring IFN release in response to possible pH change caused by intercourse or other pathological state.

To quantitatively prove the prolonged placement of PBNP in vagina shown by fluorescent imaging (Figure 6A), the intravaginal level of released IFN after intravaginal administration was evaluated by vaginal lavage and ELISA quantitation. Similar vaginal lavage methods have been used to evaluate the intravaginal placement of drug from vaginal formulations because it is a dependable and repeatable method to compare different vaginal formulations with respect to the intravaginal placement of drug.[35] Its capability

of quantitatively recovering intravaginal drug was confirmed by the detection of ~90% drug dosage when immediately conducted after intravaginal administration of IFN solution. Advantage of PBNP and PBNP-S5 was obvious at 6 hours and 24 hours after administration, which may be attributed to prolonged intravaginal placement of nanoparticles themselves and sustained release of IFN. Such a controlled and prolonged drug presence is favorable for IFN to exert its therapeutic effect.

Conclusion

In summary, good stability, easy loading and controllable release of protein therapeutics, in vitro and in vivo considerable mucoadhesive property and local safety of PBNP-S suggested it as a promising nanoscale drug delivery system, which may be used as the carrier for protein therapeutics for intravaginal administration.

Acknowledgment

Disclosure

The authors report no conflicts of interest in this work.

References

1. das Neves J, Nunes R, Machado A, Sarmento B. Polymer-based nanocarriers for vaginal drug delivery. *Adv Drug Deliv Rev*. 2015;92:53–70.
2. Kammona O, Kiparissides C. Recent advances in nanocarrier-based mucosal delivery of biomolecules. *J Control Release*. 2012;161(3):781–794.
3. Li HS, Shin MK, Singh B, et al. Nasal immunization with mannan-decorated mucoadhesive HPMCP microspheres containing ApxIIA toxin induces protective immunity against challenge infection with *Actinobacillus pleuropneumoiae* in mice. *J Control Release*. 2016;233:114–125.
4. Sheng J, He H, Han L, et al. Enhancing insulin oral absorption by using mucoadhesive nanoparticles loaded with LMWP-linked insulin conjugates. *J Control Release*. 2016;233:181–190.
5. Jin L, Boyd BJ, White PJ, Pennington MW, Norton RS, Nicolazzo JA. Buccal mucosal delivery of a potent peptide leads to therapeutically-relevant plasma concentrations for the treatment of autoimmune diseases. *J Control Release*. 2015;199:37–44.
6. Casettari L, Illum L. Chitosan in nasal delivery systems for therapeutic drugs. *J Control Release*. 2014;190:189–200.
7. Senyigit ZA, Karavana SY, Erac B, Gursel O, Limoncu MH, Baloglu E. Evaluation of chitosan based vaginal bioadhesive gel formulations for antifungal drugs. *Acta Pharm*. 2014;64(2):139–156.
8. Joraholmen MW, Vanic Z, Tho I, Skalko-Basnet N. Chitosan-coated liposomes for topical vaginal therapy: assuring localized drug effect. *Int J Pharm*. 2014;472(1–2):94–101.

9. Salmazi R, Calixto G, Bernegossi J, Ramos MA, Bauab TM, Chorilli M. A curcumin-loaded liquid crystal precursor mucoadhesive system for the treatment of vaginal candidiasis. *Int J Nanomedicine*. 2015;10: 4815–4824.

10. Bonengel S, Bernkop-Schnurch A. Thiomers – from bench to market. *J Control Release*. 2014;195:120–129.

11. Chen Y, Qu D, Zhou J, Xia G, Liu C. A microemulsion-based delivery system for enhanced absorption of epimedium flavonoids by real-time enzymolysis and mucoadhesive strategy. *J Control Release*. 2015;213: e124–e125.

12. Meng J, Zhang T, Agrahari V, Ezoulin MJ, Youan BB. Comparative biophysical properties of tenofovir-loaded, thiolated and nonthiolated chitosan nanoparticles intended for HIV prevention. *Nanomedicine*. 2014;9(11):1595–1612.

13. Millotti G, Vetter A, Leithner K, et al. Development of thiolated poly(acrylic acid) microparticles for the nasal administration of exenatide. *Drug Dev Ind Pharm*. 2014;40(12):1677–1682.

14. Nema T, Jain A, Jain A, et al. Insulin delivery through nasal route using thiolated microspheres. *Drug Deliv*. 2013;20(5):210–215.

15. Cambre JN, Sumerlin BS. Biomedical applications of boronic acid polymers. *Polymer*. 2011;52(21):4631–4643.

16. Zhang X, Wang Y, Zheng C, Li C. Phenylboronic acid-functionalized glycopolymeric nanoparticles for biomacromolecules delivery across nasal respiratory. *Eur J Pharm Biopharm*. 2012;82(1):76–84.

17. Prosperi-Porta G, Kedzior S, Muirhead B, Sheardown H. Phenylboronic-acid-based polymeric micelles for mucoadhesive anterior segment ocular drug delivery. *Biomacromolecules*. 2016;17(4):1449–1457.

18. Li C, Liu Z, Yan X, Lu W, Liu Y. Mucin-controlled drug release from mucoadhesive phenylboronic acid-rich nanoparticles. *Int J Pharm*. 2015; 479(1):261–264.

19. Monagle J, Siu L, Worrell J, Goodchild CS, Serrao JM. A phase 1c trial comparing the efficacy and safety of a new aqueous formulation of alphaxalone with propofol. *Anesth Analg*. 2015;121(4):914–924.

20. Wu J, Bu X, Dou L, Fang L, Shen Q. Co-delivery of docetaxel and berbamine by chitosan/sulfobutylether-beta-cyclodextrin nanoparticles for enhancing bioavailability and anticancer activities. *J Biomed Nanotechnol*. 2015;11(10):1847–1857.

21. Di Gioia S, Trapani A, Mandracchia D, et al. Intranasal delivery of dopamine to the striatum using glycol chitosan/sulfobutylether-beta-cyclodextrin based nanoparticles. *Eur J Pharm Biopharm*. 2015;94: 180–193.

22. Tran K, Ha-Lien Tran P, Vo TV, Truong-DinhTran T. Design of fucoidan functionalized – iron oxide nanoparticles for biomedical applications. *Curr Drug Deliv*. 2016;13(5):774–783.

23. Wu W, Mitra N, Yan EC, Zhou S. Multifunctional hybrid nanogel for integration of optical glucose sensing and self-regulated insulin release at physiological pH. *ACS Nano*. 2010;4(8):4831–4839.

24. Zheng P, Ye C, Wang X, et al. Poly(sodium vinylsulfonate)/chitosan membranes with sulfonate ionic cross-linking and free sulfate groups: preparation and application in alcohol dehydration. *J Membr Sci*. 2016; 510:220–228.

25. Determan AS, Trewyn BG, Lin VS, Nilsen-Hamilton M, Narasimhan B. Encapsulation, stabilization, and release of BSA-FITC from polyanhy-dride microspheres. *J Control Release*. 2004;100(1):97–109.

26. Dos Ramos L, de Beer S, Hempenius MA, Vancso GJ. Redox-induced backbiting of surface-tethered alkylsulfonate amphiphiles: reversible switching of surface wettability and adherence. *Langmuir*. 2015; 31(23):6343–6350.

27. Felgueiras HP, Aissa IB, Evans MD, Migonney V. Contributions of adhesive proteins to the cellular and bacterial response to surfaces treated with bioactive polymers: case of poly(sodium styrene sulfonate) grafted titanium surfaces. *J Mater Sci Mater Med*. 2015;26(11):261.

28. Cirtiu CM, Raychoudhury T, Ghoshal S, Moores A. Systematic comparison of the size, surface characteristics and colloidal stability of zero valent iron nanoparticles pre- and post-grafted with common polymers. *Colloids Surf A Physicochem Eng Asp*. 2011;390(1–3):95–104.

29. Oh S, Wilcox M, Pearson JP, Borros S. Optimal design for studying mucoadhesive polymers interaction with gastric mucin using a quartz crystal microbalance with dissipation (QCM-D): comparison of two different mucin origins. *Eur J Pharm Biopharm*. 2015;96: 477–483.

30. Aguilar-Rosas I, Alcala-Alcala S, Llera-Rojas V, Ganem-Rondero A. Preparation and characterization of mucoadhesive nanoparticles of poly (methyl vinyl ether-co-maleic anhydride) containing glycyrrhizic acid intended for vaginal administration. *Drug Dev Ind Pharm*. 2015;41(10): 1632–1639.

31. Silva CA, Nobre TM, Pavinatto FJ, Oliveira ON Jr. Interaction of chitosan and mucin in a biomembrane model environment. *J Colloid Interface Sci*. 2012;376(1):289–295.

32. Bogataj M, Vovk T, Kerec M, Dimnik A, Grabnar I, Mrhar A. The correlation between zeta potential and mucoadhesion strength on pig vesical mucosa. *Biol Pharm Bull*. 2003;26(5):743–746.

33. Bonengel S, Jelkmann M, Oh S, Mahmood A, Ijaz M, Bernkop-Schnurch A. Charge changing phosphorylated polymers: proof of in situ mucoadhesive properties. *Eur J Pharm Biopharm*. 2016;105:203–208.

34. Palmeira-de-Oliveira R, Palmeira-de-Oliveira A, Martinez-de-Oliveira J. New strategies for local treatment of vaginal infections. *Adv Drug Deliv Rev*. 2015;92:105–122.

35. Cu Y, Booth CJ, Saltzman WM. In vivo distribution of surface-modified PLGA nanoparticles following intravaginal delivery. *J Control Release*. 2011;156(2):258–264.

Supplementary materials
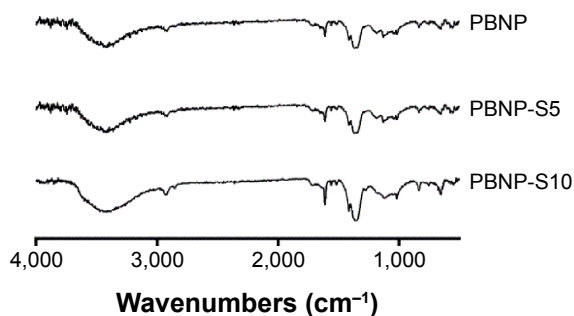
Figure S1 FT-IR spectrum of PBNP, PBNP-S5 and PBNP-S10.
Note: The absorption peaks at 1,068 cm^{-1} and 1,194 cm^{-1} in the spectrum of PBNP-S5 and PBNP-S10 can be attributed to the presence of the sulfate group.
Abbreviations: FT-IR, Fourier transform infrared spectroscopy; PBNPs, phenylboronic acid-rich nanoparticles; PBNP-S, sulfonate-modified phenylboronic acid-rich nanoparticles; PBNP-S5, PBNP-S at a weight ratio of 5%; PBNP-S10, PBNP-S at a weight ratio of 10%.

Table S1 Characterization of various PBNPs loaded with IFN-FITC

	Size		Zeta potential		Drug loading	
	Mean (nm)	**PDI**	**Mean (mV)**	**Width (mV)**	**EE (%)**	**DL (%)**
PBNP	127.0	0.212	−25.8	8.8	92.44±0.91	1.82±0.02
PBNP-S5	138.3	0.187	−30.0	6.0	93.57±1.35	1.84±0.03
PBNP-S10	159.4	0.247	−33.6	8.4	92.09±1.49	1.81±0.03

Abbreviations: PBNPs, phenylboronic acid-rich nanoparticles; IFN-FITC, fluorescein isothiocyanate-labeled interferon; PBNP-S, sulfonate-modified phenylboronic acid-rich nanoparticles; PBNP-S5, PBNP-S at a weight ratio of 5%; PBNP-S10, PBNP-S at a weight ratio of 10%; EE, encapsulation efficiency; DL, drug loading; PDI, polydispersity index.

Table S2 Characterization of various IR783-labeled PBNPs

	Size		Zeta-potential	
	Mean (nm)	**PDI**	**Mean (mV)**	**Width (mV)**
PBNP	133.7	0.207	−30.8	5.7
PBNP-S5	130.7	0.221	−37.7	11.1
PBNP-S10	131.9	0.194	−38.2	5.5

Abbreviations: PBNPs, phenylboronic acid-rich nanoparticles; PBNP-S, sulfonate-modified phenylboronic acid-rich nanoparticles; PBNP-S5, PBNP-S at a weight ratio of 5%; PBNP-S10, PBNP-S at a weight ratio of 10%; PDI, polydispersity index.

Table S3 Vaginal irritation scores for four groups

| Group	Epithelium			Mucosa									Score	Mean ± SD
	Intact	Partial exfoliation	Exudation	Vascular congestion			Edema			Leukocyte infiltration				
				Obvious	Medium	Mild	Obvious	Medium	Mild	Obvious	Medium	Mild		
	0	1	2	3	2	1	3	2	1	3	2	1		
1-1		√			√		√					√	7	6.0±1.0
1-2	√				√			√				√	5	
1-3		√			√			√				√	6	
2-1	√				√			√				√	5	4.7±0.6
2-2	√			√					√			√	5	
2-3	√				√				√			√	4	
3-1		√			√				√			√	5	4.7±0.6
3-2		√				√			√			√	4	
3-3		√			√				√			√	5	
4-1	√				√				√			√	4	4.3±0.6
4-2	√				√				√			√	4	
4-3		√			√				√			√	5	

Notes: Group 1: normal saline; Group 2: IFN; Group 3: PBNP-S; Group 4: IFN-loaded PBNP-S. 0, 1, 2 and 3 mentioned in the column head refer to score.
Abbreviations: PBNP-S, sulfonate-modified phenylboronic acid-rich nanoparticles; IFN, interferon; SD, standard deviation.
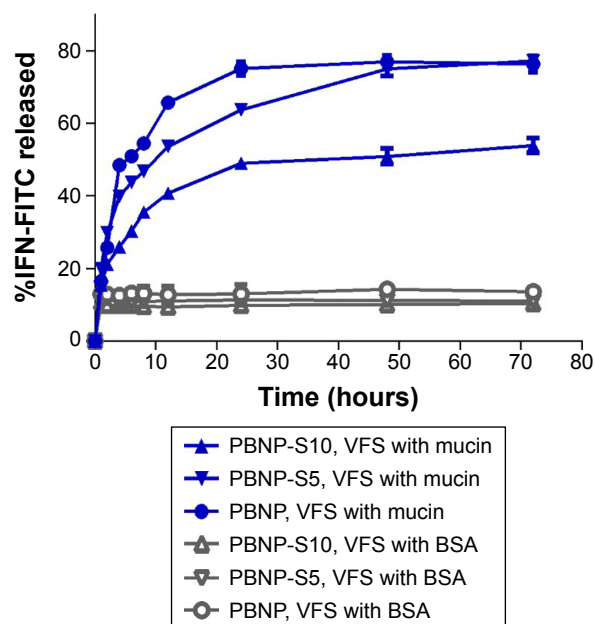
Figure S2 Drug loading and release of sulfated PBNPs with IFN-FITC as the model protein therapeutics.
Notes: Release of IFN-FITC from PBNP (circle), PBNP-S5 (inverted triangle) and PBNP-S10 (triangle) in VFS with (blue) or without mucin (gray). Data are presented as mean ± SD (n=3).
Abbreviations: PBNPs, phenylboronic acid-rich nanoparticles; IFN-FITC, fluorescein isothiocyanate-labeled interferon; PBNP-S, sulfonate-modified phenylboronic acid-rich nanoparticles; PBNP-S5, PBNP-S at a weight ratio of 5%; PBNP-S10, PBNP-S at a weight ratio of 10%; VFS, vaginal fluid simulant; SD, standard deviation.
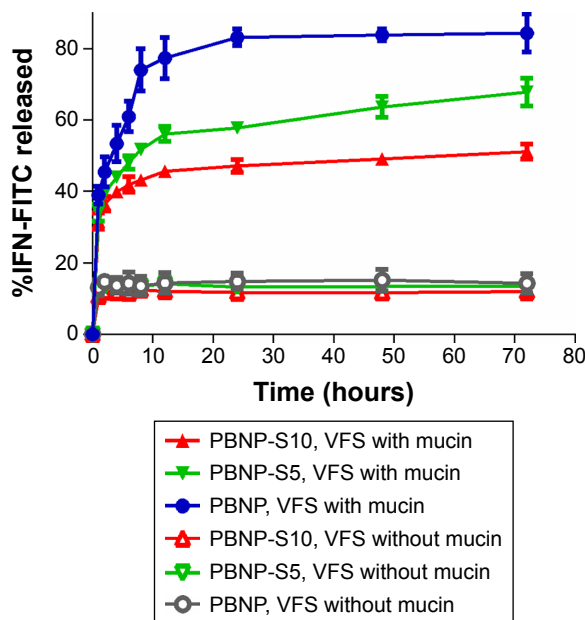
Figure S3 Release of IFN-FITC from PBNP (circle), PBNP-S5 (inverted triangle) and PBNP-S10 (triangle) in PBS (pH 6) with (filled symbols) or without (hollow symbols) mucin.
Note: Data are presented as mean ± SD (n=3).
Abbreviations: IFN-FITC, fluorescein isothiocyanate-labeled interferon; PBNPs, phenylboronic acid-rich nanoparticles; PBNP-S, sulfonate-modified phenylboronic acid-rich nanoparticles; PBNP-S5, PBNP-S at a weight ratio of 5%; PBNP-S10, PBNP-S at a weight ratio of 10%; VFS, vaginal fluid simulant; PBS, phosphate-buffered saline; SD, standard deviation.
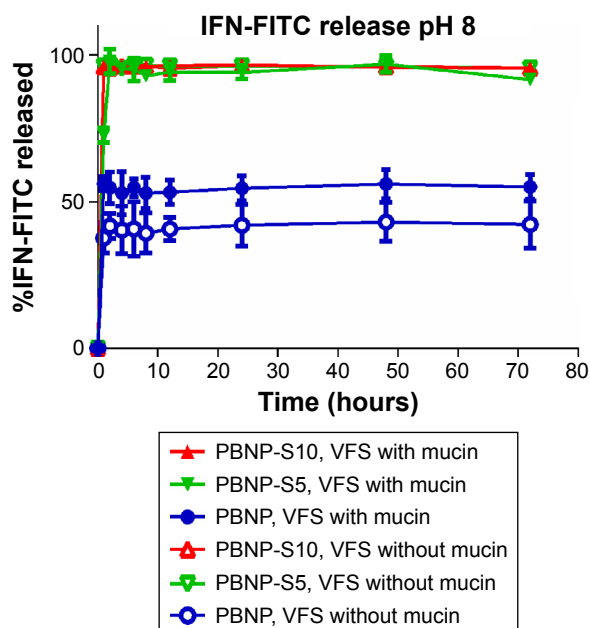
Figure S4 Release of IFN-FITC from PBNP (circle), PBNP-S5 (inverted triangle) and PBNP-S10 (triangle) in PBS (pH 8) with (filled symbols) or without (hollow symbols) mucin.
Note: Data are presented as mean ± SD (n=3).
Abbreviations: IFN-FITC, fluorescein isothiocyanate-labeled interferon; PBNPs, phenylboronic acid-rich nanoparticles; PBNP-S, sulfonate-modified phenylboronic acid-rich nanoparticles; PBNP-S5, PBNP-S at a weight ratio of 5%; PBNP-S10, PBNP-S at a weight ratio of 10%; VFS, vaginal fluid simulant; PBS, phosphate-buffered saline; SD, standard deviation.